IEEE Access
Multidisciplinary | Rapid Review | Open Access Journal

Received December 27, 2021, accepted January 15, 2022, date of publication January 26, 2022, date of current version February 8, 2022.

Digital Object Identifier 10.1109/ACCESS.2022.3146147

Power and Current Limiting Strategy Based on Droop Controller With Floating Characteristic for Grid-Connected Distributed Generations

ABDOLHOSSEIN SALEH[1], AMIR RASTEGARNIA[1], (Member, IEEE), ALI FARZAMNIA[2], (Senior Member, IEEE), AND KENNETH TEO TZE KIN[2]

[1]Department of Electrical Engineering, Malayer University, Malayer 65719-95863, Iran
[2]Faculty of Engineering, Universiti Malaysia Sabah, Kota Kinabalu 88400, Malaysia

Corresponding author: Ali Farzamnia (alifarzamnia@ums.edu.my)

This work was supported by the Research Management Center, Faculty of Engineering, Universiti Malaysia Sabah (UMS).

ABSTRACT The Grid-Connected Droop-Controlled Distributed Generations (GCDCDGs) are widely used in power systems. However, their power flow is very sensitive to the Upstream Grid (UG) frequency and voltage magnitude fluctuations. This paper focuses on the power and current limiting of inverter-interfaced GCDCDGs under UG frequency and/or voltage magnitude drops. GCDCDG output power and current increase under the UG frequency drop, and if this increase exceeds the maximum of them, current limiters are saturated and according to $P \sim \omega$ droop characteristic the GCDCDG frequency does not track the UG frequency, and this frequency difference leads to power oscillation between DG and UG and the system becomes unstable. In this paper, a new strategy based on the droop-control method is proposed to limit the output power and current of GCDCDGs without using a current limiter that realizes a stable operation under the mentioned conditions. In the proposed method instead of increasing the droop coefficients to limit P and Q at their constraints, the droop curves move down after powers and currents exceed maximum values, using two supplementary control signals. The performance of the proposed method is demonstrated with simulation results using MATLAB/Simulink environment under several case studies.

INDEX TERMS Distributed generation, droop controller, grid-connected, power and current limiting.

NOMENCLATURE

v	Output Voltage of VSC.
i	Output Current of VSC.
v_0	PC Voltage.
i_0	PC Output Current.
m	Modulating Index.
V_{DC}	VSC DC-Link Voltage.
R_f	Sum of Filter Resistance and Switches On-State Resistance.
L_l	Inter-Link Line Inductance.
R_l	Inter-Link Line Resistance.
ω_{DG}	VSC AC-Side Frequency.
ω_0	Rated Frequency.
ω_{ref}	VSC AC-Side Frequency Reference.
v_{ref}	PC Voltage Reference.
p	Instantaneous Output Active Power.
q	Instantaneous Output Reactive Power.
P_0	Rated Active Power.
Q_0	Rated Reactive Power.
P_{max}	Maximum Active Power.
Q_{max}	Maximum Reactive Power.
i_{dmax}	Maximum Active Current.
i_{dmin}	Minimum Reactive Current.
m_p	Active Current Droop Coefficient.
n_q	Reactive Current Droop Coefficient.
K_{P-id}	PI Controller Proportional Gain of Active Current.
K_{I-id}	PI Controller Integral Gain of Active Current.
K_{P-iq}	PI Controller Proportional Gain of Reactive Current.
K_{I-iq}	PI Controller Integral Gain of Reactive Current.

The associate editor coordinating the review of this manuscript and approving it for publication was Youngjin Kim.

I. INTRODUCTION

GRID-connected Distributed Generation (DGs) are extensively used to provide the demand of the consumers. These micro-power plants are usually interfaced with power inverters. These inverter-interfaced DGs to contribute in providing required power of power system which have connected to it are equipped with droop control mechanism. Droop control is usually used to enhance the stability of power systems dominated by grid-connected inverters without any communication between the different units [1]–[4]. Droop control has different forms based on the involved impedances [5]:

1) when the impedance is inductive, the droop control takes the form of $P \sim \omega$ and $Q \sim V$,
2) when the impedance is resistive, the droop control takes the form of $P \sim V$ and $Q \sim -\omega$ and,
3) when the impedance is capacitive, the droop control takes the form of $P \sim -\omega$ and $Q \sim -V$.

There are two arguments about GCDCDGs. The first is the stability of the droop control strategy which has been widely investigated in [6]–[8]. The second is to maintain the current below a given maximum limit [9]–[14]. Usually, grid-connected inverters are current-controlled, and limiting the output current of them is not difficult, while the ability to voltage regulation is a crucial aspect of power-electronics-enabled autonomous power systems [5]. It is important for a GCDCDG to be equipped with the current-limiting property where should be maintained at all times during both normal and abnormal grid conditions [10], [11], [14], [15]. Current-limiting controllers can be used to achieve the desired current limitation by triggering suitably designed protection circuits [16] or with using several Low-Voltage Ride-Through (LVRT) structures [17], [18], but these methods have difficult stability proof. External limiters and saturation units are often added into the current or voltage control loops to limit output current, but those can lead to undesired oscillations and instability [9].

A current-limiting droop controller has been proposed in [5] for single-phase grid-connected inverters that can operate under either normal or faulty grid conditions. Opposed to the conventional current-limiting methods, the current limitation in this reference is achieved without external limiters, and the controller guarantees system stability. In [22] a PV-based grid-forming inverter with a modified droop control has been considered to operate under abnormal grid voltage conditions. The proposed approach in [22] realizes current-limiting control with LVRT capabilities. A unified current-limiting control scheme for grid-connected inverters under both normal and faulty grids with a simplified voltage support mechanism has been developed in [23]. This paper focuses on the current limiting of GCDCDGs in GCMGs while UG frequency and/or voltage magnitude drop. In this paper, a new strategy based on the droop-control method is proposed to limit the output currents of GCDCDGs without using current limiters which realizes a stable operation under the above-mentioned conditions.

The main features of the proposed strategy are summarized as follows:

- power and current limiting are simultaneously occurred under UG frequency and voltage magnitude drops
- conventional current limiter which leads to instability has been deleted.
- the system has a stable operation while powers and currents are limited.
- static and dynamic load switching can not disturb performance of this limiting strategy.

The rest of the paper is divided as follows. Section II explains GCDCDG unit and its controller. Section III presents a mathematic model of the proposed droop-control based current limiting strategy. In section IV, time-domain simulation studies have been represented and finally, the conclusions are drawn in Section V.

II. GCDCDG STRUCTURE AND ITS CONTROLLERS

A typical inverter-based GCDCDG and its controllers are shown in Fig. 1. The internal controller regulates the LCL filter capacitor voltage magnitude and frequency (ω_{DG}) at their given references where are produced by the droop controller. The internal controller is based on the PI controller that has been proposed in [21]–[23]. This controller regulates control variables in dq reference frame and uses the output currents of the DG as feed-forward signals to better regulation. Fig. 2 shows the block diagram of the used internal controller. The proposed droop-control based power and current limiting strategy are discussed in the next section in detail.

III. PROPOSED DROOP-CONTROL BASED CURRENT LIMITING STRATEGY

A. CONVENTIONAL DROOP-CONTROLS USED FOR GCDCDGs

Reference of the DG frequency is determined as:

$$\omega_{ref} = \omega_0 - m_p(P - P_\theta) \tag{1}$$

where P is produced by low-pass filtering of $p = \frac{3}{2} v_{od} i_{od}$ according to

$$P = \frac{\omega_c}{s + \omega_0} p \tag{2}$$

Based on (1) when the DG injects rated active power at the UG normal conditions the reference of the DG frequency is ω_0. But under the un-normal conditions when the UG frequency decreases, because of any reasons (for example suddenly increasing demanded active power or decreasing power plant productions at UG), output active power of GCDCDG begins to increasing and based on droop characteristic (1) DG frequency is decreased to DG drawn active power be proportional to capacity of it.

Reference of the DG voltage magnitude is determined as follow:

$$v_{ref} = v_0 - n_q(Q - Q_0) \tag{3}$$

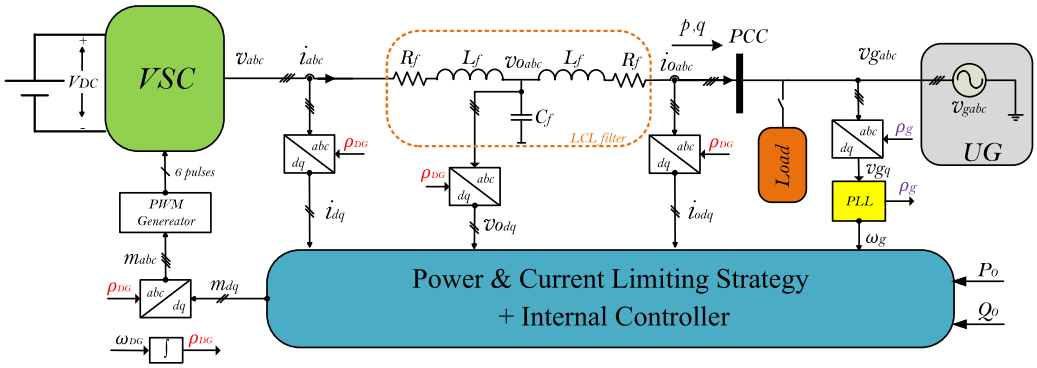

FIGURE 1. The schematic diagram of the GCDCDG system.

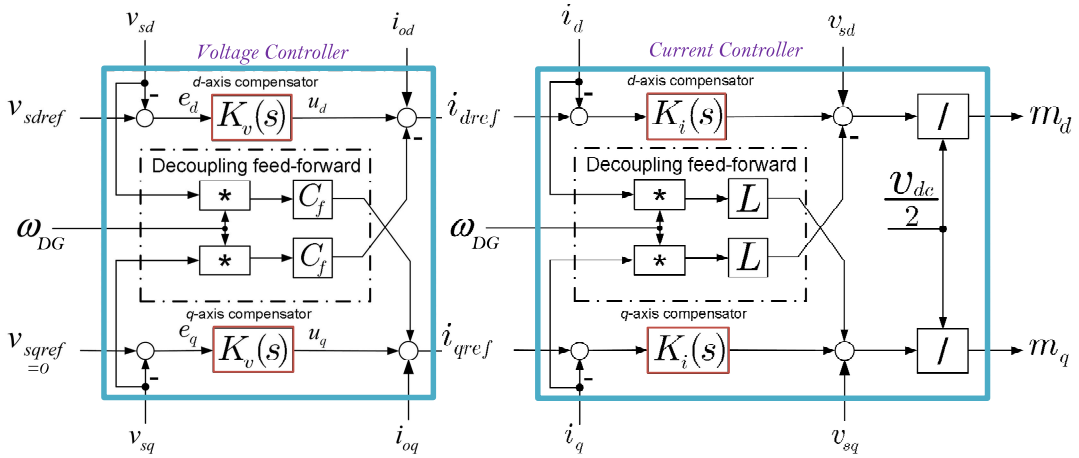

FIGURE 2. Block diagram of GCDCDG internal controller.

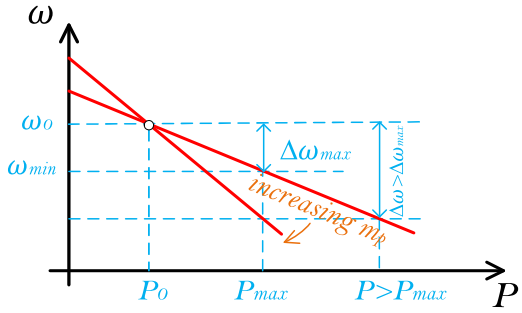

FIGURE 3. $P-\omega$ droop characteristic.

where Q is produced by low-pass filtering of $q = -\frac{3}{2}v_{od}i_{oq}$ according to:

$$Q = \frac{\omega_c}{(s+\omega_c)}q \tag{4}$$

Based on (3) when the DG injects rated reactive power at the UG normal conditions the reference of the DG voltage magnitude is v_0. But under the abnormal conditions when the UG voltage magnitude decreases, because of any reasons (for example short circuit faults at UG), output reactive power of GCDCDG begins to increase, and based on droop characteristic (3) DG voltage magnitude is decreased to DG drawn reactive power be proportional to the capacity of it.

Under the above UG conditions, if UG frequency and/or voltage magnitude drop be large values, output powers of the GCDCDG maybe exceed the maximum of them. One solution to limit the output powers to maximum values is using current limiters to limit i_{od} and i_{oq} to maximum values. This method in order to limit output reactive power performs correctly, but in output active power limiting a problem occurs. If UG frequency decreases, i_{od} increases, and if this increasing exceeds the maximum of i_{od}, the current limiter is saturated and according to $P \sim \omega$ droop characteristic (Fig. 3) the GCDCDG frequency does not track the UG frequency and this frequency difference, leads to power oscillation between DG and UG and the system becomes unstable. Also, increasing m_p to limit the output active power due to stability limit is not possible [9].

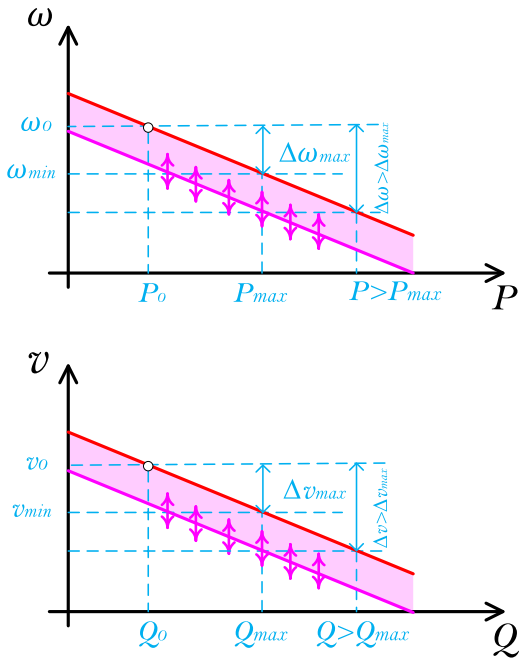

FIGURE 4. (Top) $P-\omega$ and (bottom) $Q-v$ droop characteristic.

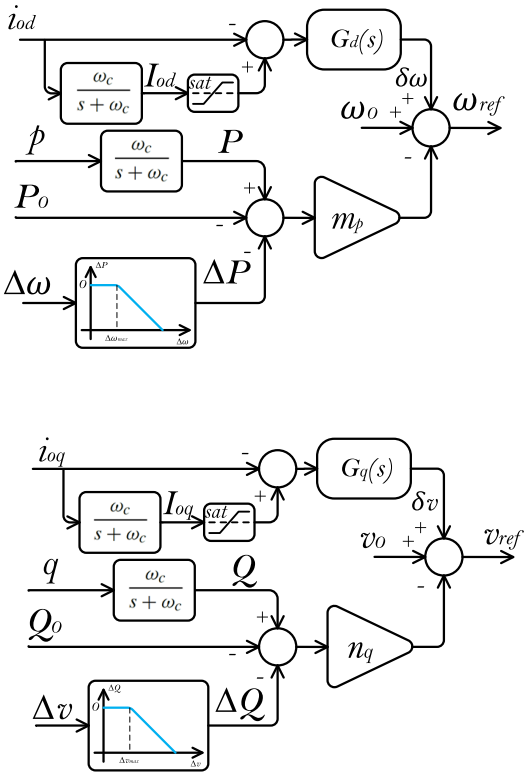

FIGURE 5. Block diagrams of proposed droop-control based power and current limiting strategy: (top) P and I_{od} limiter and (bottom) Q and I_{oq} limiter.

To overcome the above-mentioned problems the proposed unified droop-control based current limiting strategy will be described as follows.

B. PROPOSED STRATEGY

In the proposed strategy, same as the conventional method the drop of DG frequency and voltage magnitude is based on P and Q increasing, respectively. Thus (1) and (3) are used as previously used. According to (1) and (3), in steady-state, minimum values of ω_{ref} and v_{ref} occur at the maximum value of P and Q, respectively.

$$\omega_{min} = \omega_0 - m_p(P_{max} - P_0) \tag{5}$$
$$v_{min} = v_0 - n_q(Q_{max} - Q_0) \tag{6}$$

Thus, using (5) and (6), a maximum drop from rated values of frequency and voltage magnitude that protection strategy is not active until they are

$$\Delta_{max} = \omega_0 - \omega_{min} = m_p(P_{max} - P_0) \tag{7}$$
$$\Delta_{max} = v_0 - v_{min} = n_q(Q_{max} - Q_0) \tag{8}$$

According to $P \sim \omega$ and $Q \sim v$ droop characteristics in Fig. 4, if frequency and voltage magnitude drops be greater than $\Delta\omega_{max}$, Δv_{max}, P and Q will be exceed the maximum values in steady-state, respectively. In the proposed method instead of increasing the droop coefficients to limit P and Q at their constraints, the droop curves move down after exceeding $\Delta\omega_{max}$ and Δv_{max}, using two supplementary control signals as follows:

$$\omega_{ref} = \omega_0 - m_p(P - P_0 - \Delta P) \tag{9}$$
$$v_{ref} = v_0 - n_q(Q - Q_0 - \Delta Q) \tag{10}$$

where ΔP and ΔQ are calculated so that P and Q limit to P_{max} and Q_{max} even after increasing of $\Delta\omega$ and Δv from their maximums, respectively. Thus:

$$\Delta\omega = m_p(P_{max} - P_0 - \Delta P) \tag{11}$$
$$\Delta v = n_q(Q_{max} - Q_0 - \Delta Q) \tag{12}$$

Note that (11) and (12) can be rewritten as

$$\Delta P = \begin{cases} -\dfrac{1}{m_p}\Delta\omega + (P_{max} - P_0) & \Delta\omega > \Delta\omega_{max} \\ 0 & \Delta\omega \le \Delta\omega_{max} \end{cases} \tag{13}$$

$$\Delta Q = \begin{cases} -\dfrac{1}{n_q}\Delta v + (Q_{max} - Q_0) & \Delta v > \Delta v_{max} \\ 0 & \Delta v \le \Delta v_{max} \end{cases} \tag{14}$$

where (13) and (14) limit P and Q to maximum values. Also, to ensure that in a transient state, instantaneous active and reactive power (i.e. p and q) and currents i_{od} and i_{oq} do not exceed their boundary values, two other supplementary control signals are added to (11) and (12), as

$$\omega_{ref} = \omega_0 - m_p(P - P_0 - \Delta P) + \delta\omega \tag{15}$$
$$v_{ref} = v_0 - n_q(Q - Q_0 - \Delta Q) + \delta v \tag{16}$$

where $\delta\omega$ and δv are respectively produced based on minimizing the difference between instantaneous and steady-state

TABLE 1. Parameters for DG.

Parameter	Symbol	Value
Rated power	S_n(kVA)	1.1
Rated voltage	V_n (V)	62.5
DC bus voltage	V_{DC} (V)	200
Rated frequency	f_0	50
Switching frequency	$f_{SW}(kHz)$	20
Filter inductance	L_f (mH)	1.5
Filter capacitance	C_f (μ F)	20
Filter resistance	R_f (mΩ)	1.5
Rated active power	P_0 (W)	240
Rated reactive current	Q_0 (W)	60
Maximum active current	i_{odmax} (A)	12
Minimum reactive current	i_{qdmax} (A)	-7.2
Active power droop coefficient	m_d	0.001
Reactive power droop coefficient	n_q	0.002
PI controller proportional gain of active current	K_{P-id}	0.4
PI controller integral gain of active current	K_{I-id}	0.5
PI controller proportional gain of reactive current	K_{P-iq}	-4
PI controller integral gain of reactive current	K_{I-iq}	-5
LPF cut-off frequency	ω (rad/s)	15
Interlink line resistance	R_L (Ω)	0.001
Interlink line inductance	L_L (mH)	0.001

values of i_{od} and of i_{oq} by PI controllers. These supplementary control signals are

$$\delta\omega(s) = \underbrace{\left(K_{P-id} + \frac{K_{I-id}}{S}\right)}_{G_p(s)}(I_{od} - i_{od}(s)) \tag{17}$$

$$\delta v(s) = \underbrace{\left(K_{P-iq} + \frac{K_{I-iq}}{S}\right)}_{G_q(s)}\left(I_{oq} - i_{oq}(s)\right) \tag{18}$$

where

$$I_{od} = \frac{\omega_c}{s+\omega_c} i_{od} \tag{19}$$

$$I_{oq} = \frac{\omega_c}{s+\omega_c} i_{oq} \tag{20}$$

Since steady-state values of currents are produced by low pass filtering instantaneous value of them and have not predefined values, to ensure that i_{od} and i_{oq} do not exceed their boundary values, I_{od} and I_{oq} signals are saturated at them. In the proposed scheme the steady-state power control is based on droop control, thus the current saturation mechanism does not deal with system instability. Fig. 5 shows a block diagram of the proposed droop-control based power and current limiting strategy.

IV. TIME-DOMAIN SIMULATION RESULTS

In this section, the performance of the proposed strategy is investigated under four various case studies. The proposed droop-control based power and current limiting strategy is applied to a GCDCDG. The detailed switched model of the system is simulated using MATLAB/Simulink environment. A Diagram of this system has been shown in Fig. 1 in which the UG block is replaced with a series inter-link line and ideal voltage source. Parameters of this DG are given in Table 1. In these cases, until $t = 2$ sec, DG operates in its rated conditions i.e. $V_{od} \approx 51$ V, $f_o = 50$ Hz, $P_o = 235$ W,

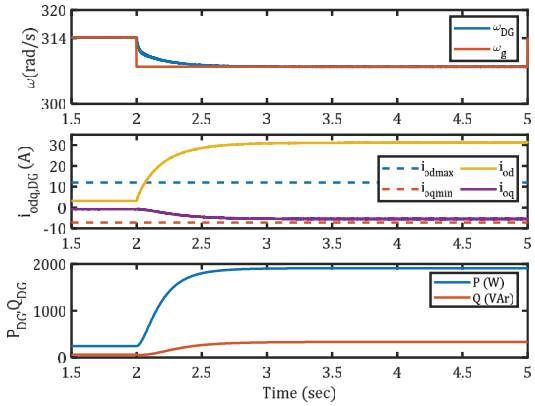

FIGURE 6. Simulation results in UG frequency drop without using current limiting strategy.

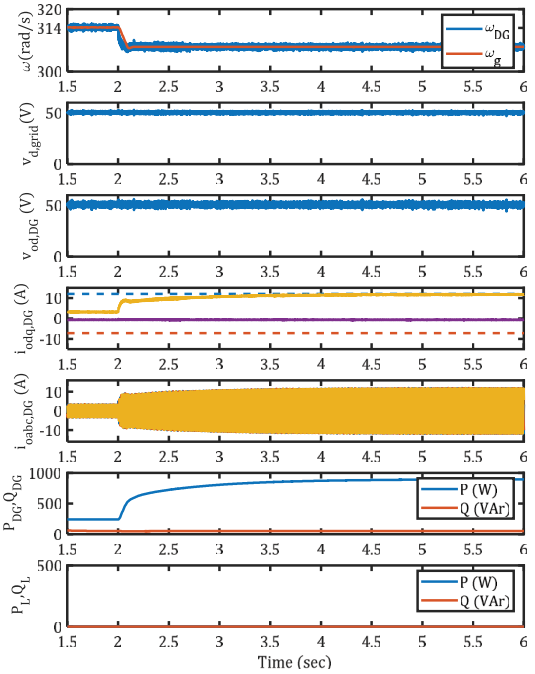

FIGURE 7. Simulation results in UG frequency drop under proposed current limiting strategy.

$Q_o \approx 59.6$ VAr, $i_{od} = 3.068$ A and $i_{oq} \approx -0.779$ A. Also, the line to line voltage of $UG(V_{gL-L})$ is 61.24 V.

A. CASE STUDY 1: UG FREQUENCY DROP

At $t = 2$ sec the UG frequency drops to 49 Hz ($\omega_g = 307.867$ rad/s). Since the UG voltage phase lag from the voltage phase of DG, active power injection from DG to UG begins to increase and this is because of i_{od} increasing. As shown in Fig. 6, 1 Hz Frequency drop is large and i_{od} exceeds the maximum of it if the current limiting strategy is not used. Also, the injected active power reaches about 2 kW which is lonely greater than the rated power of the DG. To limit the active current i_{od} to its maximum value, the proposed strategy is applied and the simulation results are shown in Fig.7. As can be see, i_{od} limited to $i_{odmax} = 12$ A.

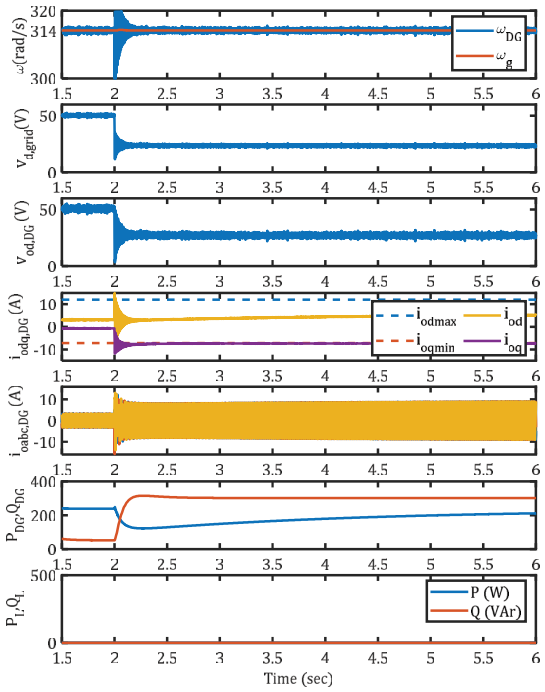

FIGURE 8. Simulation results in UG voltage magnitude drop under proposed current limiting strategy.

In steady-state, injected active and reactive power under this frequency drop are about 900 W and 60 VAr respectively where result $S \approx 902$ VA.

B. CASE STUDY 2: UG VOLTAGE MAGNITUDE DROP

In this study at $t = 2$ sec the UG voltage magnitude drops to 27.56 $V_{(L-L)}$ from 62.5 $V_{(L-L)}$ i.e. 44 percent decrease at PCC. As shown in Fig. 8, i_{oq} decreases and is limited to the minimum value of it i.e. -7.2 A. Because of this reactive current decrease, reactive power injection increases and in steady-state raised to 301 VAr. The steady-state value of i_{od} and ω_{DG} remain without changes but since the proposed strategy decreases LCL filter capacitor bus voltage magnitude to control and limit i_{oq}, the output active power decreases during transient state and in steady-state restores to the previous value. Fig. 9 represents i_{oq} when the proposed current limiting strategy is not used. In this study, 56 percent decrease for UG voltage magnitude is applied at PCC. As can be seen from Fig. 9, i_{oq} exceeds boundary and decreases to about -12 A if conventional droop without current limiter is used.

C. CASE STUDY 3: DROP IN UG FREQUENCY AND VOLTAGE MAGNITUDE AND BALANCED LOAD SWITCHING

To show the ability of the proposed current limiting strategy, UG frequency and voltage magnitude are simultaneously decreased to 49 Hz and 27 $V_{(L-L)}$ (i.e. $V_{d,gerid} = 22$), respectively. Fig. 10 shows simulation results in this case study. After $t = 2$ sec, when frequency and voltage magnitude are decreased, i_{od} and i_{oq} move to boundary values and in steady-state reach to them and active and reactive powers

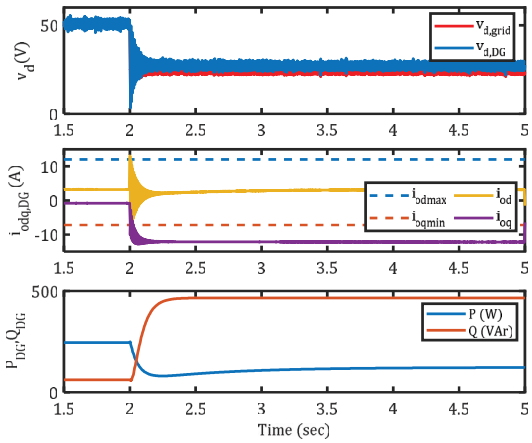

FIGURE 9. Simulation results in UG magnitude voltage drop without using current limiting strategy.

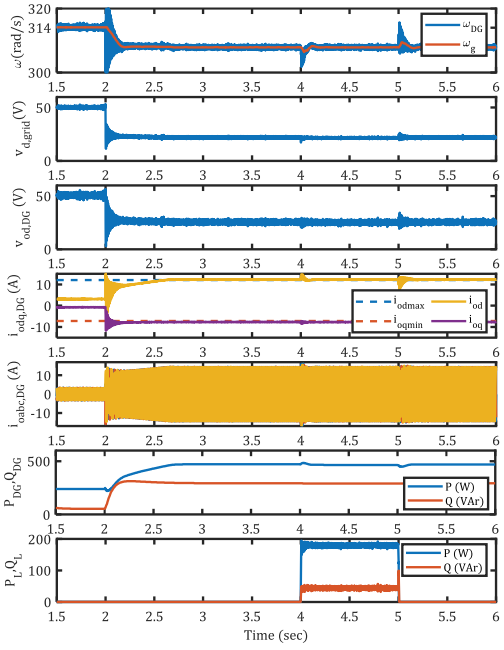

FIGURE 10. Simulation results in UG frequency and voltage magnitude drop and balanced load switching.

are 471 W and 293 VAr, respectively. Between $t = 4$ sec and $t = 5$ sec, a three-phase balanced load is connected at PCC and starts to drawing current. For this load $P_L = 174$ W and $Q_L = 45$ VAr. As can be seen in Fig. 10, output currents of the DG are controlled and do not exceed boundary values, and are limited under the proposed strategy. The required power of the load is provided from the grid under this abnormal condition.

D. CASE STUDY 4: DROP IN UG FREQUENCY AND VOLTAGE MAGNITUDE AND INDUCTION MOTOR LOAD SWITCHING

This case study is the same as case study 3, but, instead of a three-phase balanced load, an induction motor with

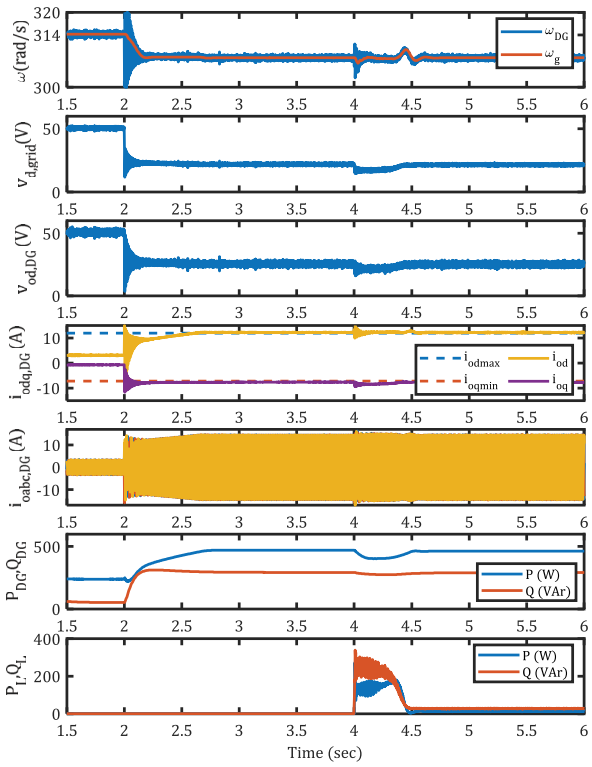

FIGURE 11. Simulation results in UG frequency and voltage magnitude drop and induction motor load switching.

$S = 200$ VA as a dynamic load is connected at $t = 4$ sec. Simulation results are given in Fig. 11. Results show that the proposed strategy control output currents and does not permit to currents raise over the boundary values.

Remark 1: The performance of the system under the conventional droop controller has been shown in Fig.6 and Fig. 9. As can be seen in these figures output powers of the grid-connected DG exceed limits under the UG frequency and voltage magnitude drops while under the proposed strategy even if local static and dynamic load are switched, output powers don't exceed their limits. Thus these results can be sufficient to show the advantages of the proposed method.

V. CONCLUSION

This paper presents a power and current limiting strategy of GCDCDG under UG frequency and/or voltage magnitude reduction. The proposed new strategy which is based on the droop-control method limits the output power and currents of GCDCDGs without using current limiters that realize a stable operation under the above-mentioned conditions. The performance of the proposed method has been demonstrated by simulation results using MATLAB/Simulink environment under several case studies for an individual GCDCDG. The performance of the proposed strategy has been evaluated under UG frequency and voltage magnitude drops and for a severe condition while these reductions occur local RL balanced and three-phase induction motor load have been switched on. Results of studies indicate that the proposed strategy will be perfectly able to limit the output currents of the grid-connected DGs under frequency and/or voltage magnitude reductions.

REFERENCES

[1] Z. Zhang, C. Dou, D. Yue, B. Zhang, S. Xu, T. Hayat, and A. Alsaedi, "An event-triggered secondary control strategy with network delay in islanded microgrids," *IEEE Syst. J.*, vol. 13, no. 2, pp. 1851–1860, Jun. 2019.

[2] M. E. Meral and D. Çelík, "A comprehensive survey on control strategies of distributed generation power systems under normal and abnormal conditions," *Annu. Rev. Control*, vol. 47, pp. 112–132, Jan. 2019.

[3] Y. Gupta, S. Doolla, K. Chatterjee, and B. C. Pal, "Optimal DG allocation and Volt–Var dispatch for a droop-based microgrid," *IEEE Trans. Smart Grid*, vol. 12, no. 1, pp. 169–181, Jan. 2021.

[4] N. M. Dehkordi and S. Z. Moussavi, "Distributed resilient adaptive control of islanded microgrids under sensor/actuator faults," *IEEE Trans. Smart Grid*, vol. 11, no. 3, pp. 2699–2708, May 2020.

[5] Q. Zhong and G. C. Konstantopoulos, "Current-limiting droop control of grid-connected inverters," *IEEE Trans. Ind. Electron.*, vol. 64, no. 7, pp. 5963–5974, Oct. 2017.

[6] M. Eskandari and A. V. Savkin, "On the impact of fault ride-through on transient stability of autonomous microgrids: Nonlinear analysis and solution," *IEEE Trans. Smart Grid*, vol. 12, no. 2, pp. 999–1010, Mar. 2021.

[7] Y. Peng, Z. Shuai, X. Liu, Z. Li, J. M. Guerrero, and Z. J. Shen, "Modeling and stability analysis of inverter-based microgrid under harmonic conditions," *IEEE Trans. Smart Grid*, vol. 11, no. 2, pp. 1330–1342, Mar. 2020.

[8] M. Ganjian-Aboukheili, M. Shahabi, Q. Shafiee, and J. M. Guerrero, "Seamless transition of microgrids operation from grid-connected to islanded mode," *IEEE Trans. Smart Grid*, vol. 11, no. 3, pp. 2106–2114, May 2020.

[9] Y. Geng, L. Zhu, X. Song, K. Wang, and X. Li, "A modified droop control for grid-connected inverters with improved stability in the fluctuation of grid frequency and voltage magnitude," *IEEE Access*, vol. 7, pp. 75658–75669, 2019.

[10] H. Yazdanpanahi, Y. W. Li, and W. Xu, "A new control strategy to mitigate the impact of inverter-based DGs on protection system," *IEEE Trans. Smart Grid*, vol. 3, no. 3, pp. 1427–1436, Sep. 2012.

[11] D. M. Vilathgamuwa, P. C. Loh, and Y. Li, "Protection of microgrids during utility voltage sags," *IEEE Trans. Ind. Electron.*, vol. 53, no. 5, pp. 1427–1436, Oct. 2006.

[12] D. Çelík and M. E. Meral, "A flexible control strategy with overcurrent limitation in distributed generation systems," *Int. J. Electr. Power Energy Syst.*, vol. 104, pp. 456–471, Jan. 2019.

[13] S. Dedeoglu, G. C. Konstantopoulos, and A. G. Paspatis, "Grid-supporting three-phase inverters with inherent root mean square current limitation under balanced grid voltage sags," *IEEE Trans. Ind. Electron.*, vol. 68, no. 11, pp. 11379–11389, Nov. 2021.

[14] H. J. Laaksonen, "Protection principles for future microgrids," *IEEE Trans. Power Electron.*, vol. 25, no. 12, pp. 2910–2918, Dec. 2010.

[15] X. Guo, W. Liu, X. Zhang, X. Sun, Z. Lu, and J. M. Guerrero, "Flexible control strategy for grid-connected inverter under unbalanced grid faults without PLL," *IEEE Trans. Power Electron.*, vol. 30, no. 4, pp. 1773–1778, Apr. 2015.

[16] Z. Chen, X. Pei, M. Yang, L. Peng, and P. Shi, "A novel protection scheme for inverter-interfaced microgrid (IIM) operated in islanded mode," *IEEE Trans. Power Electron.*, vol. 33, no. 9, pp. 7684–7697, Sep. 2018.

[17] I. Sadeghkhani, M. E. H. Golshan, J. M. Guerrero, and A. Mehrizi-Sani, "A current limiting strategy to improve fault ride-through of inverter interfaced autonomous microgrids," *IEEE Trans. Smart Grid*, vol. 8, no. 5, pp. 2138–2148, Sep. 2017.

[18] L. Zhou, A. Swain, and A. Ukil, "Reinforcement learning controllers for enhancement of low voltage ride through capability in hybrid power systems," *IEEE Trans. Ind. Informat.*, vol. 16, no. 8, pp. 5023–5031, Aug. 2020.

[19] Y. Jiang, X. Li, C. Qin, X. Xing, and Z. Chen, "Improved particle swarm optimization based selective harmonic elimination and neutral point balance control for three-level inverter in low-voltage ride-through operation," *IEEE Trans. Ind. Informat.*, vol. 18, no. 1, pp. 642–652, Jan. 2022.

[20] A. G. Paspatis, G. C. Konstantopoulos, and J. M. Guerrero, "Enhanced current-limiting droop controller for grid-connected inverters to guarantee stability and maximize power injection under grid faults," *IEEE Trans. Control Syst. Technol.*, vol. 29, no. 2, pp. 841–849, Mar. 2021.
[21] M. B. Delghavi and A. Yazdani, "A unified control strategy for electronically interfaced distributed energy resources," *IEEE Trans. Power Del.*, vol. 27, no. 2, pp. 803–812, Apr. 2012.
[22] J. Rocabert, A. Luna, F. Blaabjerg, and P. Rodríguez, "Control of power converters in AC microgrids," *IEEE Trans. Power Electron.*, vol. 27, no. 11, pp. 4734–4749, Nov. 2012.
[23] M. E. Meral and D. Çelik, "Proportional complex integral based control of distributed energy converters connected to unbalanced grid system," *Control Eng. Pract.*, vol. 103, pp. 1–13, Oct. 2020.

ABDOLHOSSEIN SALEH was born in Nahavand, Hamedan, Iran, in December, 1987. He received the Ph.D. degree in electrical engineering from Bu-Ali Sina University, Hamedan, in 2019. He is currently an Assistant Professor with Malayer University, Malayer, Hamedan. His research interests include power quality, switching power converters, distributed generation, and microgrids and their control.

AMIR RASTEGARNIA (Member, IEEE) received the Ph.D. degree in electrical engineering from the University of Tabriz, Tabriz, Iran, in 2011. In 2011, he joined the Department of Electrical Engineering, Malayer University, as an Assistant Professor. His current research interests include theory and methods for adaptive and statistical signal processing, distributed adaptive estimation, and signal processing for communications.

ALI FARZAMNIA (Senior Member, IEEE) received the B.Eng. degree in electrical engineering (telecommunication engineering) from the Islamic Azad University of Urmia, Iran, in 2005, the M.Sc. degree in electrical engineering (telecommunication engineering) from the University of Tabriz, in 2008, and the Ph.D. degree in electrical engineering (telecommunication engineering) from Universiti Teknologi Malaysia (UTM), in 2014. He has been a Senior Lecturer (Assistant Professor) in the Electrical and Electronic Engineering Program, Faculty of Engineering, Universiti Malaysia Sabah (UMS), since 2014. He has secured several research grants with numerous dedicated collaborative research partners. He is a Chartered Engineer (CEng.) in the United Kingdom. His research interests include wireless communication, signal processing, network coding, information theory, and bio-medical signal processing. He is a member of IET.

KENNETH TEO TZE KIN received the B.Eng. (Hons.), M.Sc., and Ph.D. degrees in electrical and electronic engineering from the University of Leicester, U.K., and Universiti Malaysia Sabah (UMS), Malaysia, respectively. He is currently a Senior Lecturer of electrical and electronic engineering with the Faculty of Engineering, UMS. His research activities, for the past 20 years, are focused on precision optimization and artificial intelligence in the field of smart energy, intelligent transportation, precision automation, and analytical mechatronics and biomedical science. He pioneered the Modelling, Simulation and Computing Laboratory (mscLab) founded in 2009. With the expertise in dynamic modeling and optimization, his team had evolved from 3C (computation, communication, and control) toward PC (precision computing) especially in the area of evolutionary computation, deep learning, and semantic agents. He is currently leading the Artificial Intelligence Research Unit and the Electrical and Electronic Engineering Program at UMS. He is committed to IEEE activities as an Advisor of IEEE Student Branch (UMS) and Committee of Malaysia Sabah Subsection.